

## Hybrid energy storage system optimal sizing for urban electrical bus regarding battery thermal behavior

Si Mohamed Faresse, Mohamed Assini, Abdallah Saad

Laboratory of Electrical Systems and Energy, National Higher School of Electricity and Mechanics (ENSEM), Hassan II University of Casablanca, Morocco

---

### Article Info

#### Article history:

Received April 19, 2019

Revised Dec 31, 2019

Accepted Jan 8, 2020

#### Keywords:

Battery

Battery thermal behavior

Buck-boost DC/DC converter

Fully electrical bus

Hybrid energy storage system

Supercapacitor

### ABSTRACT

This paper proposes an algorithm for sizing the hybrid energy storage system of an urban electrical bus regarding battery thermal behavior. The aim of this study is to get the supercapacitors optimal contribution part in the hybrid energy storage system to keep the battery temperature within its allowable limit. A semi-active parallel topology that uses supercapacitors as a main source of energy is considered. According to the bus mechanical parameters and the ARTEMIS driving cycle, the power and energy demand are calculated. Using mathematical models for the battery, supercapacitors and DC-DC converter, several simulations are performed for different hybridization percentages. While observing the evolution of battery temperature, the most favorable hybridization percentage is defined.

Copyright © 2020 Institute of Advanced Engineering and Science.  
All rights reserved.

---

### Corresponding Author:

Si Mohamed Faresse,  
Laboratory of Electrical Systems and Energy,  
Department of Electrical Engineering,  
National Higher School of Electricity and Mechanics,  
Hassan II University of Casablanca,  
El Jadida Road, km 7, Casablanca, Morocco.  
Email: sm.faresse@gmail.com

---

### NOMENCLATURE

$V_{batt}$	Battery voltage (V)
$E_0$	Constant voltage (V)
$K$	Polarization constant (Ah <sup>-1</sup> )
$i^*$	Low frequency current dynamics (A)
$I$	Battery current (A)
$it$	Extracted capacity (Ah)
$Q$	Maximum battery capacity (Ah)
$A$	Exponential voltage (V)
$B$	Exponential capacity (Ah <sup>-1</sup> )
$R_b$	Battery internal resistance (Ω)
$T_{ref}$	Nominal ambient temperature (K)
$T$	Cell or internal temperature (K)
$T_a$	Ambient temperature (K)
$\partial E/\partial T$	Reversible voltage temperature coefficient (V/K)
$\alpha$	Arrhenius rate constant for the polarization resistance
$\beta$	Arrhenius rate constant for the internal resistance
$\Delta Q/\Delta T$	Maximum capacity temperature coefficient (Ah/K)

C	Nominal discharge curve slope (V/Ah)
$R_{th}$	Thermal resistance, cell to ambient ( $^{\circ}\text{C}/\text{W}$ )
$t_c$	Thermal time constant, cell to ambient (s)
$P_{loss}$	Overall heat generated during charge/discharge (W)
$i_{sc}$	Supercapacitor current (A)
$V_{sc}$	Supercapacitor voltage (V)
$R_{sc}$	Supercapacitor total resistance (ohms)
$N_e$	Number of layers of electrodes
$N_p$	Number of parallel supercapacitors
$N_s$	Number of series supercapacitors
$Q_T$	Electric charge (C)
R	Ideal gas constant
d	Molecular radius
$T_o$	Operating temperature (K)
E	Permittivity of material
$\epsilon_0$	Permittivity of free space
$A_i$	Interfacial area between electrodes and electrolyte ( $\text{m}^2$ )
c	Molar concentration ( $\text{mol}/\text{m}^3$ )
F	Faraday constant
$F_{tr}$	Tractive force (N)
$F_{aero}$	Aerodynamic drag (N)
$F_{rr}$	Rolling resistance (N)
$F_i$	Inertial force (N)
$F_{gr}$	Grade force (N)
$\rho$	Air density
$C_d$	Air drag coefficient
$A_f$	Front Surface ( $\text{m}^2$ )
V	Velocity (m/s)
m	Total mass (kg)
g	Gravitational force ( $\text{m}\cdot\text{s}^{-2}$ )
$\theta$	Drag angle (rad)
$C_r$	Rolling friction factor
a	Acceleration ( $\text{m}\cdot\text{s}^{-2}$ )
$r_w$	Wheel radius (m)
$i_d$	Gear transmission ratio
$\eta_d$	Gear transmission efficiency
$\Omega$	Angular speed ( $\text{rad}\cdot\text{s}^{-1}$ )
P	Power (W)
T	Torque (N.m)

## 1. INTRODUCTION

The first autonomous electric buses were equipped with batteries as a source of energy [1]. These batteries have some disadvantages, namely a too slow dynamic [2] and overheating problem [3,4]. The combination of batteries and supercapacitors (SC) is the suitable solution for electric vehicle [5]. This combination has complementary qualities and provides an excellent solution that can increase dynamic behavior and cover a wide range of power and energy requirements and it was demonstrated that this combination has lower battery costs [6], a general increase in battery life and higher overall system efficiency [7]. Starting from the observation that battery buses are used almost exclusively in urban areas rather than for long-distance transport. The urban transport has relatively short intervals between recharging possibilities. Externally based energy storage on SC can be a solution since they can charge much faster than conventional batteries [8].

In the literature, most of the reported works focus solely on the electrical behavior of hybrid energy storage system (HESS). While the behavior of the battery temperature in this kind of application has not yet been treated. All HESS sizing methodologies for electric buses do not considerate the battery temperature evolution. And to remedy to this problem, supercapacitors oversizing is done.

Obviously, HESS topologies are very diverse, depending mainly on the type of application [9]. For the studied case, the selected topology will use the SC as the main source [10]. Our study is to redo this dimensioning while considering the temperature of the battery to choose the optimal capacity value of

supercapacitors. In this study, an algorithm is proposed to define the minimum SC energy part in the hybrid storage system for electrical bus to maintain the battery in its permissible temperature zone. In this work we neglected the regenerative braking energy. The suggested algorithm is applied to "Irizar ie" bus, with a total mass of 16000 kg following an ARTEMIS driving cycle on a working day of 24 round trips. Total energy required is calculated. Then, capacity part of each element is defined and for each percentage of hybridization the temperature evolution is determined using battery model which consider temperature effect.

This paper is organized as follows: After the Introduction is given in the first section, the System Description and Modeling are introduced in section 2. The Research Method is presented in section 3. Then, the Electric Bus Energy Storage Sizing is addressed in section 4. Finally, section Simulation Results develops battery thermal behavior for different percentage of hybridization. The conclusions are given in the last section.

## 2. DESCRIPTION AND SYSTEM MODELING

### 2.1. Hybrid energy storage system topologies

Four possible topologies [11,12,13] for the HESS are presented below:

#### 2.2.1. Parallel passive topology

The basic passive parallel hybrid configuration is shown in Figure 1, the SC pack and the batteries are directly connected in parallel to the load. Because of the direct connection, the SC pack basically acts as a low-pass filter. The main advantage is the ease of implementation and no complicated control device required. The disadvantage of this configuration is that the power sharing between the battery and the SC pack is uncontrolled and dictated solely by the parasitic elements. Also the DC bus voltage is not regulated and varies depending on the voltage range of the batteries, which influences the design load.

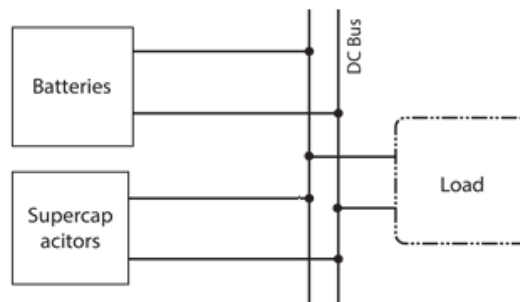


Figure 1. Passive parallel hybrid configuration

#### 2.2.2. Parallel active topology

The multi-converter configuration uses two separate bidirectional back-boost converters as shown in Figure 2. The batteries and SC pack voltage can be kept lower than the DC bus voltage, less balancing problems. The voltage of the SC pack can vary in a wide range so that the capacitor is fully used. The advantage of this configuration is that the power of the batteries and SC pack can be individually controlled according to their state of charge and power requirements. The disadvantage of this topology is the increase in the number of components and the cost.

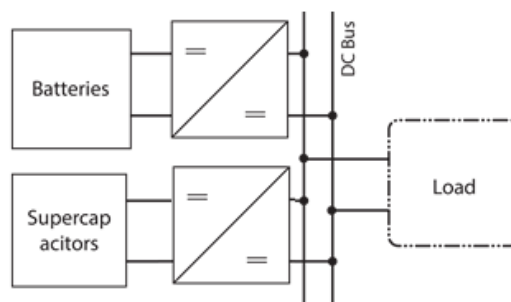


Figure 2. Active parallel hybrid configuration

### 2.2.3. Parallel semi active battery/supercapacitor topology

The Parallel Semi Active battery/supercapacitor configuration is illustrated in Figure 3. In this configuration, the batteries voltage can be kept lower or higher than the SC pack voltage. The SC pack is connected to the DC bus and works directly as a low-pass filter. But the power of the batteries is uncontrollable. The control strategy applied to this topology allows the DC link voltage to vary in a range so that SC pack energy can be used more efficiently.

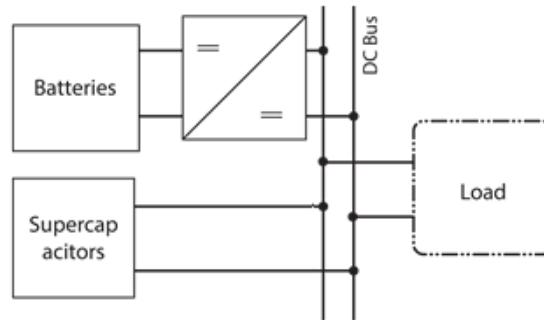


Figure 3. Battery/Supercapacitor parallel configuration

### 2.2.4. Parallel semi active supercapacitor/battery topology

Figure 4 shows the diagram of the HESS configuration using a bi-directional buck-boost converter for the SC pack interface, the SC pack voltage can be used in a wider range. This configuration has a single controlled power source. However, the bidirectional converter must be oversized to handle the power of the SC pack. In addition, the nominal voltage of the SC pack may be lower. The batteries are connected directly to the DC bus. Therefore, the DC bus voltage is fixed.

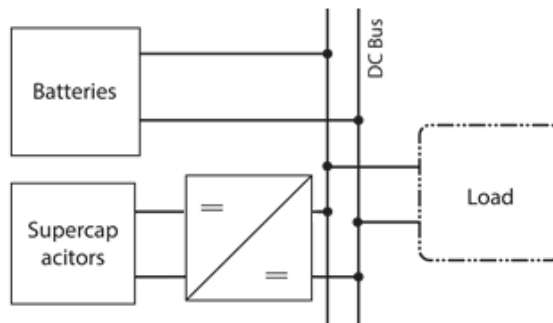


Figure 4. Supercapacitor/battery parallel configuration

## 2.2. Electric bus system description

Our goal is to use SC pack as the main power source for the bus because of their power density and their dynamic, which will be recharged at each bus stop to solve the problem of their low energy density. The battery will intervene in case of the SC discharge. The proper configuration is the Parallel Active Topology. It allows the maximum use of stored energy in SC while keeping the nominal voltage of the load. Due to its cost, the parallel active configuration will be discarded. Due to its advantages [14] the Parallel Semi Active Supercapacitor/Battery Topology will be used in the bus, where the overall system is shown in Figure 5 [15,16].

The supercapacitor (SC1) that can produce and absorb peak power is the main element of the energy storage system of the electric urban bus, which can be charged by the other SC in the bus stop. The battery will be used in extreme conditions when the supercapacitor is almost exhausted. The general structure of the charging station at the bus stop [17] is illustrated in Figure 6. The electric urban bus SC can be charged by (SC2) supercapacitor through a DC/DC converter at each bus stop when passengers get on and off. SC2 can be charged by the power grid via an AC/DC converter between them with a lower power density before the next bus arrives. With this method, the impact of surge on the power distribution network can be avoided.

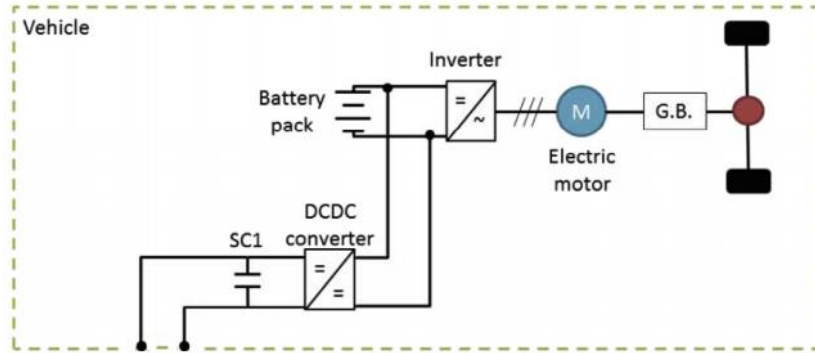


Figure 5. Scheme of electric bus storage system

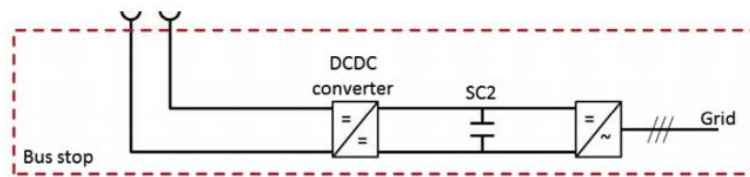


Figure 6. Scheme of electric bus powertrain

### 2.3. Hybrid energy storage system modeling

#### 2.3.1. Battery model

In this work, we use MATLAB model for lithium-ion battery. Two models will be presented below (with and without temperature effect). For each model the discharge equation will be presented. The lithium-ion battery model without temperature effect is given as [18]:

$$V_{batt}(it, i^*, i) = E_0 - K \frac{Q}{Q - it} \cdot i^* - K \frac{Q}{Q - it} \cdot it + A \cdot \exp(-B \cdot it) - R_b \cdot i \quad (1)$$

The impact of temperature on the model parameters is represented bellow [19]:

$$V_{batt}(it, i^*, i, T, T_a) = E_0(T) - K(T) \frac{Q(T_a)}{Q(T_a) - it} \cdot (i^* + it) + A \cdot \exp(-B \cdot it) - C \cdot it + R_b(T) \cdot i \quad (2)$$

with:

$$E_0(T) = E_0|_{T_{ref}} + \frac{\partial E}{\partial T} (T - T_{ref}) \quad (3)$$

$$K(T) = K|_{T_{ref}} \cdot \exp(\alpha \cdot (\frac{1}{T} - \frac{1}{T_{ref}})) \quad (4)$$

$$Q(T_a) = Q|_{T_a} + \frac{\Delta Q}{\Delta T} (T_a - T_{ref}) \quad (5)$$

$$R_b(T) = R_b|_{T_{ref}} \cdot \exp(\beta \cdot (\frac{1}{T} - \frac{1}{T_{ref}})) \quad (6)$$

The cell or internal temperature T, at any given time t, is expressed as:

$$T(t) = L^{-1}(\frac{P_{loss} R_{th} + T_a}{1 + s \cdot t_c}) \quad (7)$$

where:

$$P_{loss} = (E_0(T) - V_{batt}(T)) \cdot i + \frac{\partial E}{\partial T} \cdot i \cdot T \tag{8}$$

**2.3.2. Supercapacitor model**

The SC is an emerging technology in the field of energy storage systems. Energy storage is performed by the means of static charge rather than of an electro-chemical process that is inherent to the battery [20]. The supercapacitor model used in this work is a generic MATLAB model parameterized to represent most popular types of SC [21]. The SC output voltage is expressed using a Stern equation as:

$$V_{sc} = \frac{N_s Q_T d}{N_p N_e \epsilon \epsilon_0 A_i} + \frac{2 N_e N_s R T_0}{F} \sinh^{-1} \left( \frac{Q_T}{N_p N_e^2 A_i \sqrt{8 R T_0 \epsilon \epsilon_0 C}} \right) - R_{sc} \cdot i_{sc} \tag{9}$$

With :  $Q_T = \int i_{sc} dt$

**2.3.3. DC/DC converter model**

DC/DC converters can be represented by two types of models, namely the switching models and the average value models. Switching models are mainly used for design purposes and to study the types of pulse width modulated systems with respect to switching harmonics and losses. These models require a low sampling time to observe all the switching actions, which makes the simulation very long.

On the contrary, medium-valued models take less time because the switches are replaced by controlled voltage/current sources. The switching harmonics are not represented, but all the dynamics of the converter are maintained, which makes these models attractive, because a longer sampling time can be used. Models of DC/DC converters of average value are used in this paper, as shown in Figure 7. The design of the control loops is performed taking into account the dynamics of the model [22].

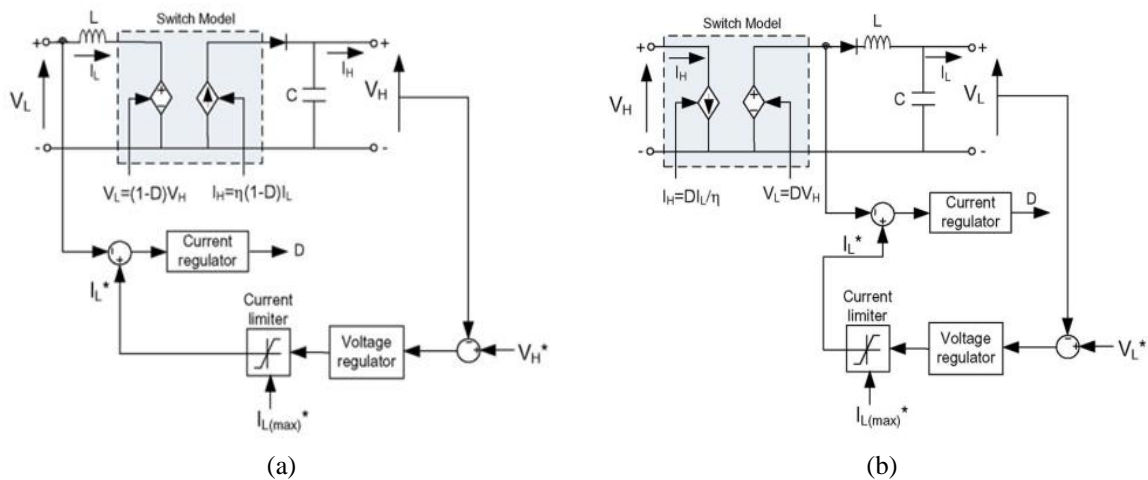


Figure 7. DC/DC Converter Model, (a) Boost type. (b) Buck type

**3. RESEARCH METHOD**

In this article, the choice of the hybrid energy storage system elements for a totally electric bus is carried out according to the diagram represented in Figure 8. The illustrated approach consists in determining all the energies consumed between two consecutive stops on the total path of the bus. These energies are normally determined from the mechanical characteristics of the bus and the bus driving cycle. Then choose a supercapacitor pack to ensure the minimum of calculated energies. Next, determine the battery capacity to ensure the power supply of the bus during a working day, knowing that the supercapacitors pack, which will be recharged at each bus stop, will provide partial or total power between two consecutive stops.

Subsequently, use the model developed under MATLAB/Simulink, which uses the parallel semi-active topology Supercapacitor/Battery, with the model of the battery which considers the temperature effect, by applying the chosen value of the supercapacitors and battery. Then observe the evolution of the battery temperature during a day of operation. If the observed temperature exceeds the battery permissible value, the energy value just above the energy used for the supercapacitor must be chosen from the energies already calculated. And repeat the same algorithm until finding the optimum value of HESS elements.

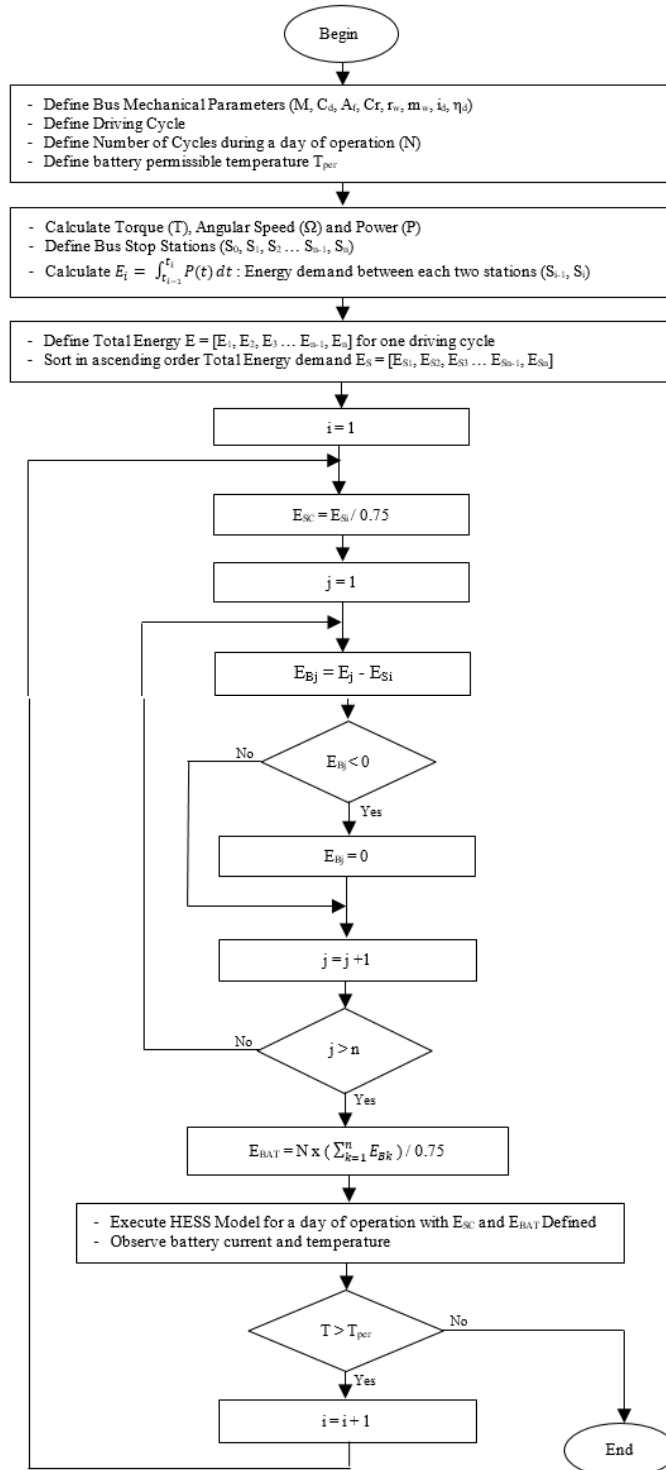


Figure 8. Flow chart of the proposed algorithm

#### 4. ELECTRIC BUS ENERGY STORAGE SIZING

The objective of this part is to size the energy storage system of a fully electrical bus from well-defined specifications.

##### 4.1. Bus mechanical parameters

The main mechanical characteristics of the chosen bus are summarized in Table 1. The vehicle is constructed applying the body of "Irizar ie" bus with a new rear transmission ratio of 8.

Table 1. Bus mechanical parameters

Parameters	Symbol	Values
Total mass (fully loaded)	M	16 000 kg
Air drag coefficient	$C_d$	0.65
Front surface	$A_f$	8 m <sup>2</sup>
Rolling friction factor	$C_r$	0.008
Wheel radius	$r_w$	0.48 m
Wheel mass	$m_w$	50 kg
Gear transmission ratio	$i_d$	8 : 1
Gear transmission efficiency	$\eta_d$	0.97

##### 4.2. Driving cycle

The chosen driving cycle is ARTEMIS Urban [23] illustrated in Figure 9.

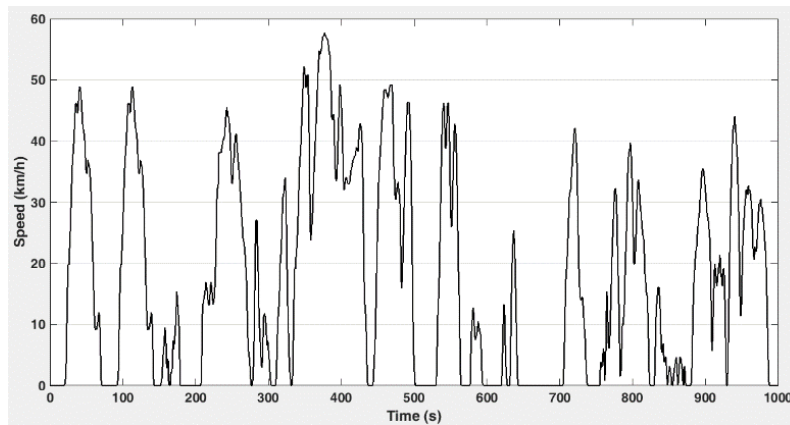


Figure 9. ARTEMIS urban driving cycle

The main features of this cycle are:

Distance : 4870 m  
 Duration : 993 sec  
 Average speed : 17.6 km/h  
 Maximum speed : 57.7 km/h

##### 4.3. Motor torque, angular speed and power calculation

The rotational speed and power demand for the powertrain and the torque demand to overcome friction forces (rolling and air resistance) are depicted in Figure 10.

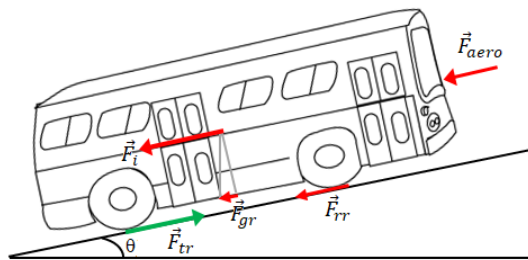


Figure 10. Forces applied to the bus



The bus traction force required is given by this equation [24-26]:

$$F_{tr} = F_{aero} + F_{rr} + F_i + F_{gr} \quad (10)$$

where:

$$F_{aero} = \frac{1}{2} \rho C_d A_f V^2 \quad (11)$$

$$F_{rr} = m g \sin(\theta) \quad (12)$$

$$F_{gr} = m g C_r \quad (13)$$

$$F_i = a m_i \quad (14)$$

$$m_i = 1.04 m \quad (15)$$

$$a = \frac{F_{tr} - (F_{aero} + F_{rr} + F_{gr})}{m_i} \quad (16)$$

From the tractive force and the linear velocity, we can deduce the motor torque, angular velocity and Power:

$$T = \frac{F_{tr} r_w}{i_d \eta_d} \quad (17)$$

$$\Omega = \frac{v i_d}{r_w} \quad (18)$$

$$P = T \cdot \Omega \quad (19)$$

Figures 11, 12, and 13 show respectively the calculated torque, angular velocity and power required for an ARTEMIS driving cycle.

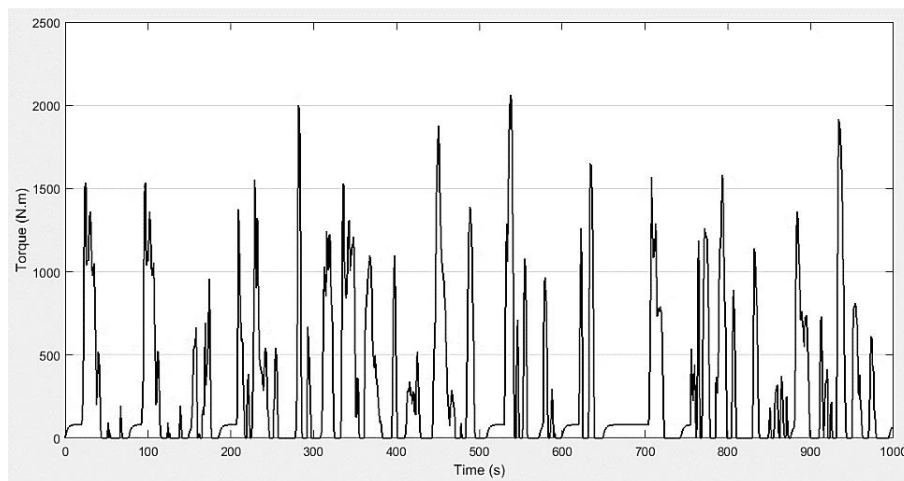


Figure 11. Bus motor torque

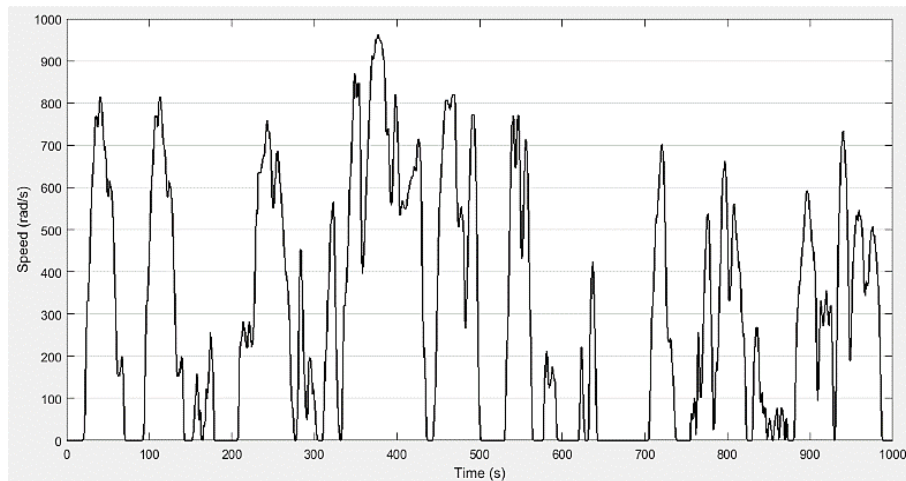


Figure 12. Bus motor angular velocity

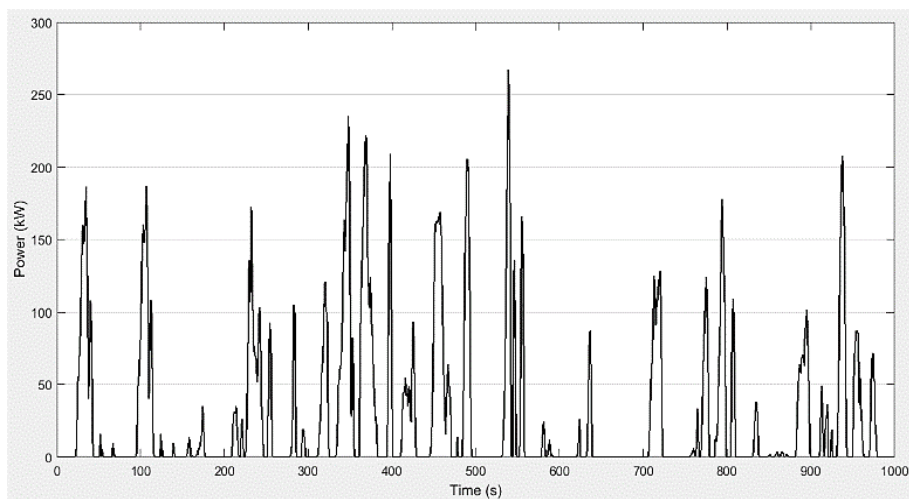


Figure 13. Bus motor power

#### 4.4. Bus energy autonomous calculation

We define eight stations in the given driving cycle, the total driving range is 4870 m. The duration and the demand energy between two successive stations are calculated and listed in Table 2. The total energy demand for 1000 seconds ARTEMIS driving cycle is approximately 7.6 kWh. We estimate that the route between two bus terminals is two ARTEMIS cycles followed by a 15 minute break (each trip will last 2900 seconds). For a day operation, we define 24 round trips or 48 ARTEMIS cycles. The total energy required for a day is 364 kWh.

Table 2. Energy consumption between two successive bus stops

Bus stop N°	Duration (s)	Energy (Wh)
1	0 → 72	559
2	73 → 180	604
3	181 → 503	3617
4	504 → 566	616
5	567 → 596	25
6	597 → 644	100
7	645 → 739	383
8	740 → 989	1686

## 5. SIMULATION RESULTS

All simulation tests are executed with different operating conditions in MATLAB/Simulink environment. The simulations have been carried out during 69 600 s which represent the bus day operation time. In this study, we proposed eight simulation tests that represent the battery temperature evolution for each HESS combination given by Table 3. The aim is to find the best configuration with minimum SC capacity, to ensure the autonomous and the battery permissible temperature. The chosen battery parameters are summarized in Table 4. For each simulation performed, we present the battery current draw between two bus terminals that lasts about 2000 seconds followed by 900 seconds rest. The evolution of the temperature corresponding to this current draw during a day of operation are presented respectively in Figures 14-20 for different HESS combinations given by Table 3.

Table 3. HESS combinations

Case N°	SC capacity (F)	SC energy (Wh)	Battery energy (kWh)	Battery energy (Ah)
1	0	0	485	871
2	4	34	472	848
3	16	133	439	788
4	60	511	330	592
5	86	744	274	492
6	93	802	262	470
7	146	1264	217	389
8	259	2248	124	222
9	556	4823	0	0

Table 4. Battery parameters

Parameter	Value
Type	Lithium-ion
Nominal Voltage (V)	557
Initial State of Charge (%)	100
Battery Response Time (s)	30
Cut-off Voltage (V)	378
Fully Charged Voltage	587
Internal Resistance (Ohms)	0.00504
Initial cell temperature (deg. C)	20
Nominal ambient temperature T1 (deg. C)	20
Thermal resistance, cell-to-ambient (deg. C/W)	0.4
Thermal time constant, cell-to-ambient (s)	20000

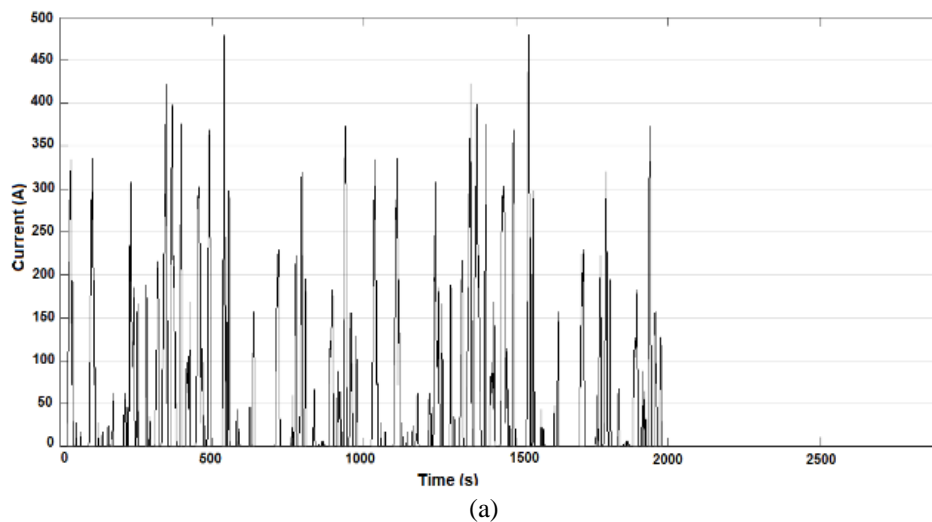


Figure 14. (a) Battery current

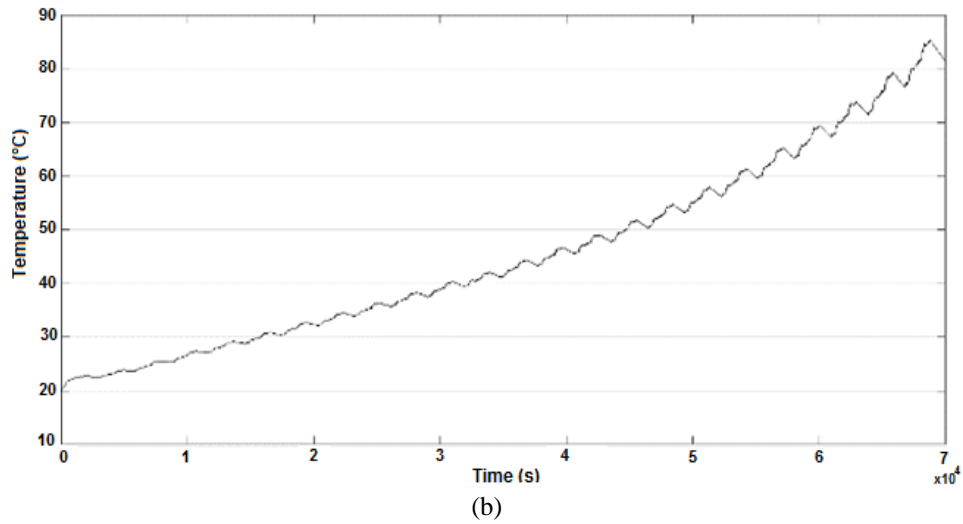


Figure 14. (b) Battery temperature, ( $E_{Batt} = 871 \text{ Ah}$  and  $E_{SC} = 0 \text{ Wh}$ ) (*continue*)

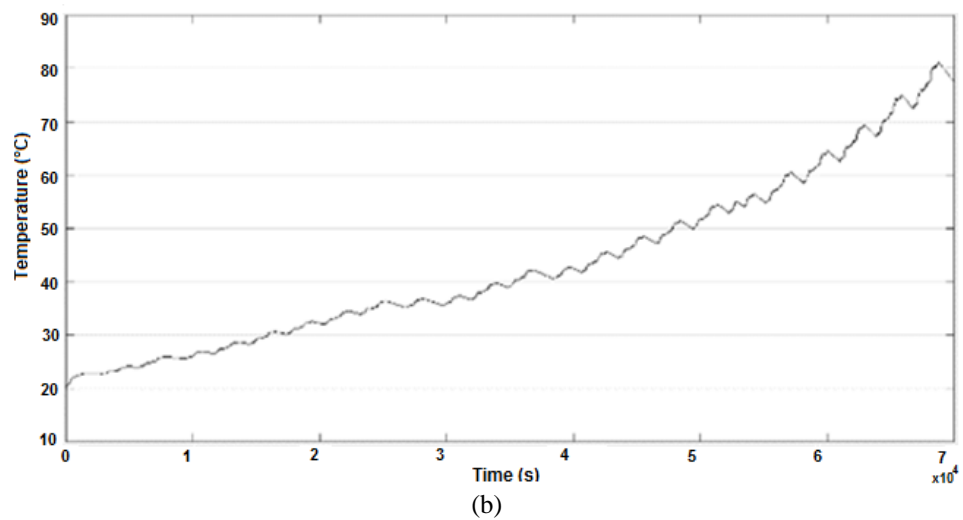
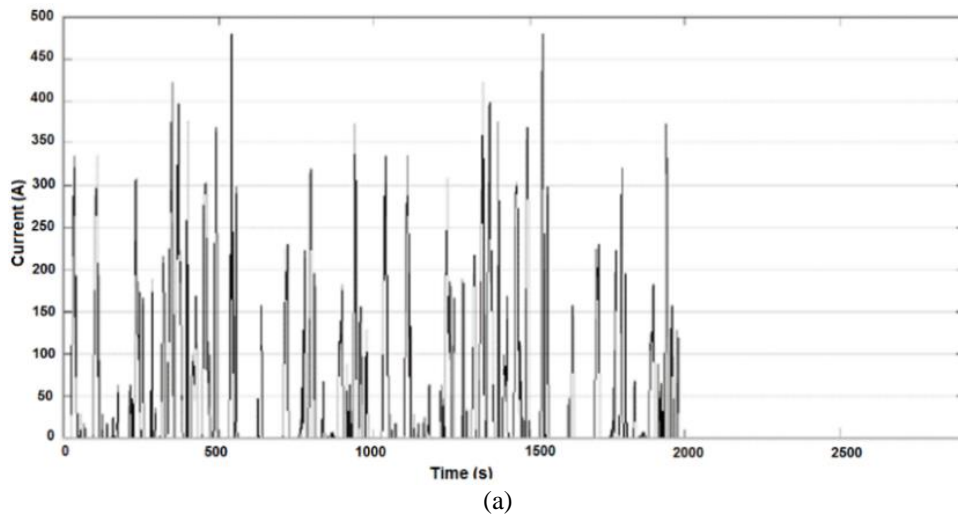
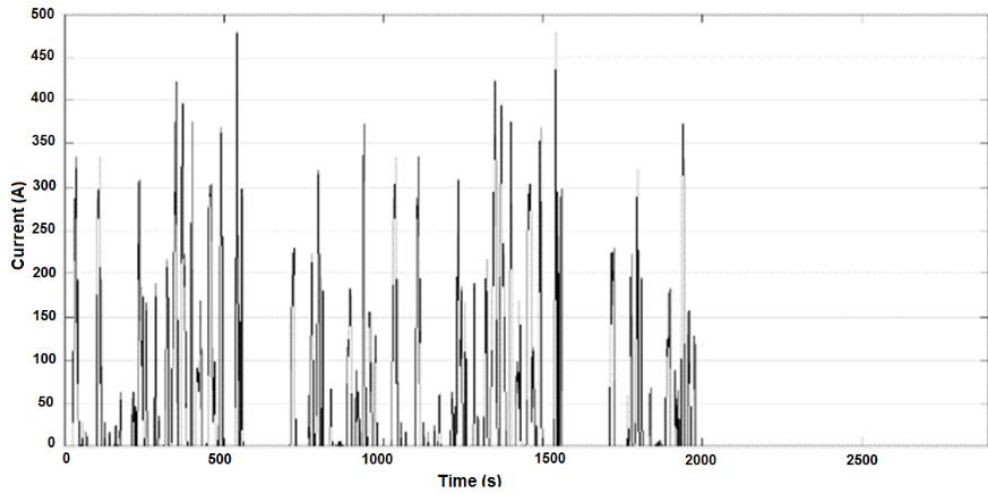
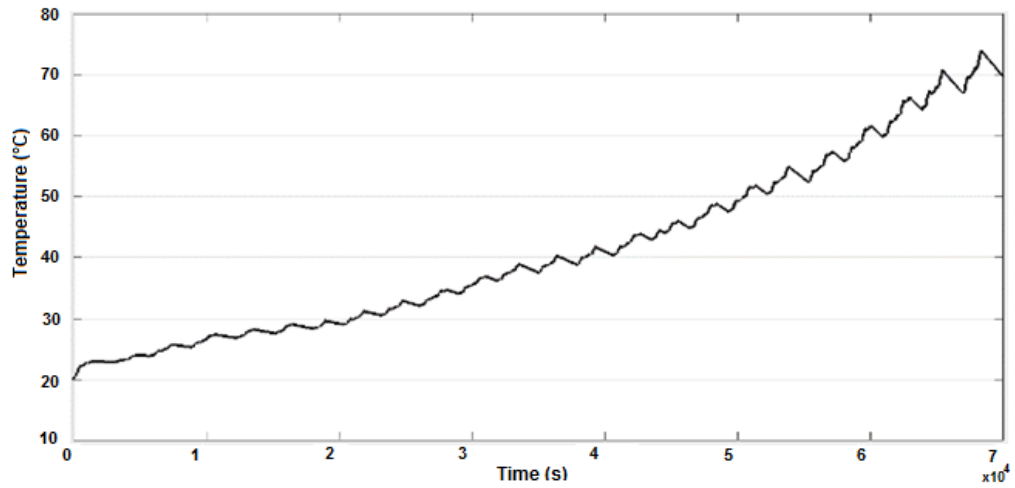


Figure 15. (a) Battery current, (b) Battery temperature, ( $E_{Batt} = 848 \text{ Ah}$  and  $E_{SC} = 34 \text{ Wh}$ )

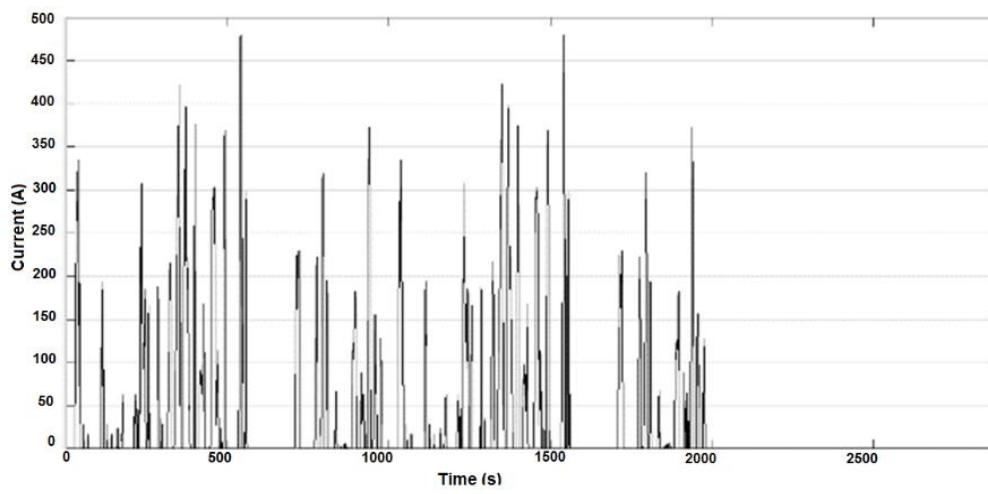


(a)



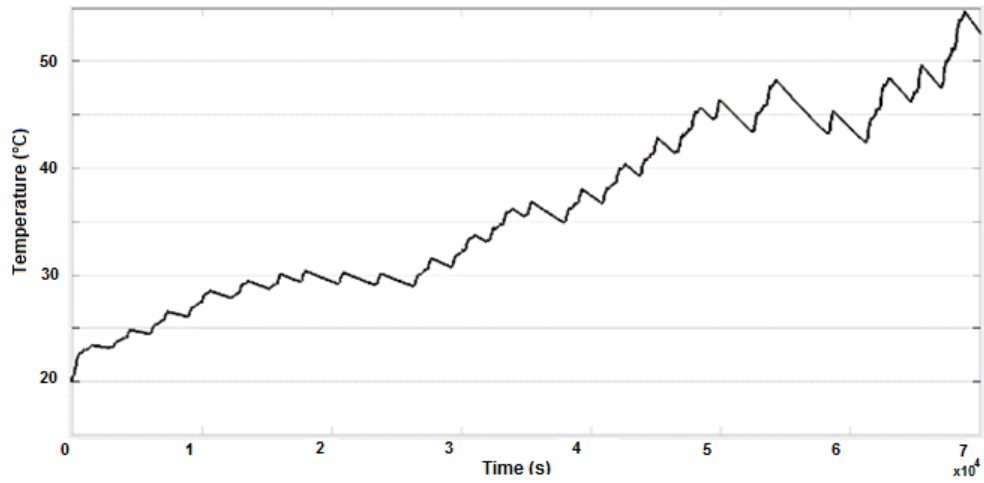
(b)

Figure 16. Battery current (a) and Battery temperature (b) ( $E_{Batt} = 788Ah$  and  $E_{SC} = 133Wh$ )



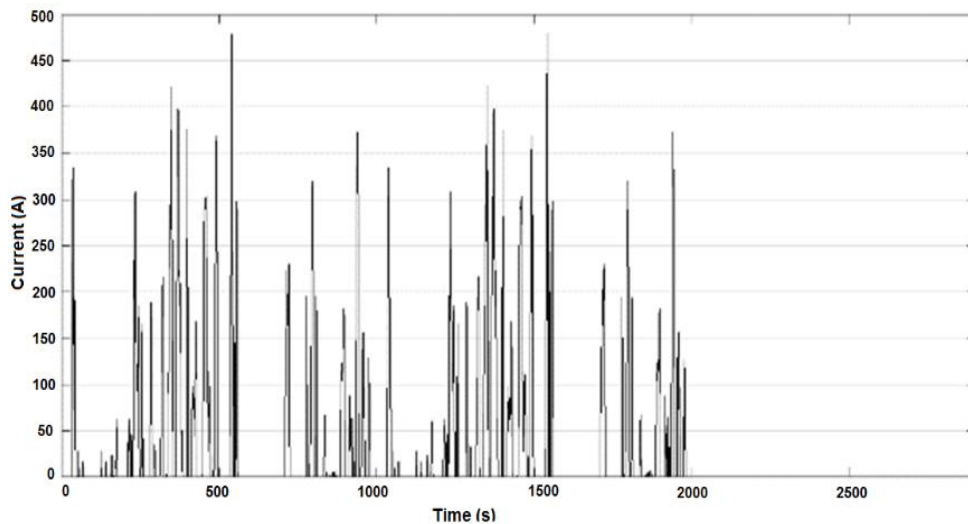
(a)

Figure 17. Battery current (a) Battery temperature

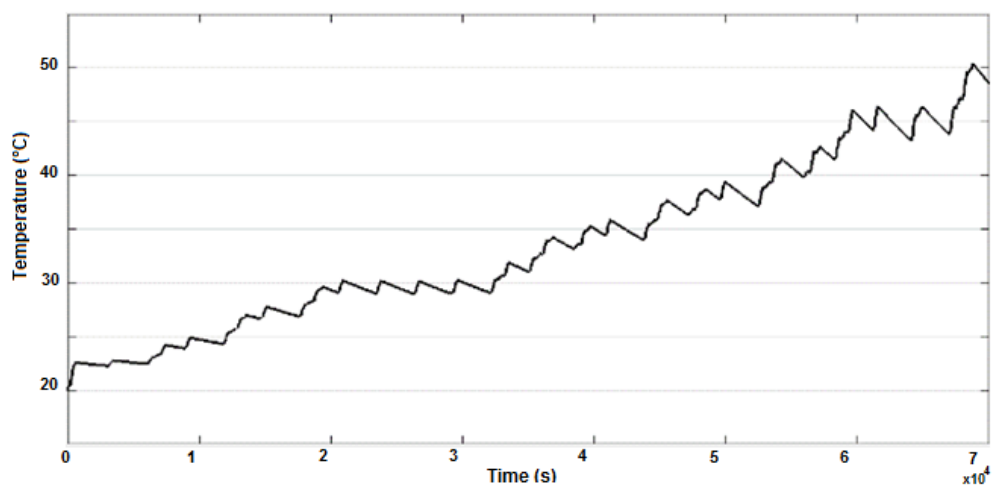


(b)

Figure 17. Battery current (b) ( $E_{Batt} = 592Ah$  and  $E_{SC} = 511Wh$ ) (continue)



(a)



(b)

Figure 18. Battery current (a) and Battery temperature (b) ( $E_{Batt} = 492Ah$  and  $E_{SC} = 744Wh$ )

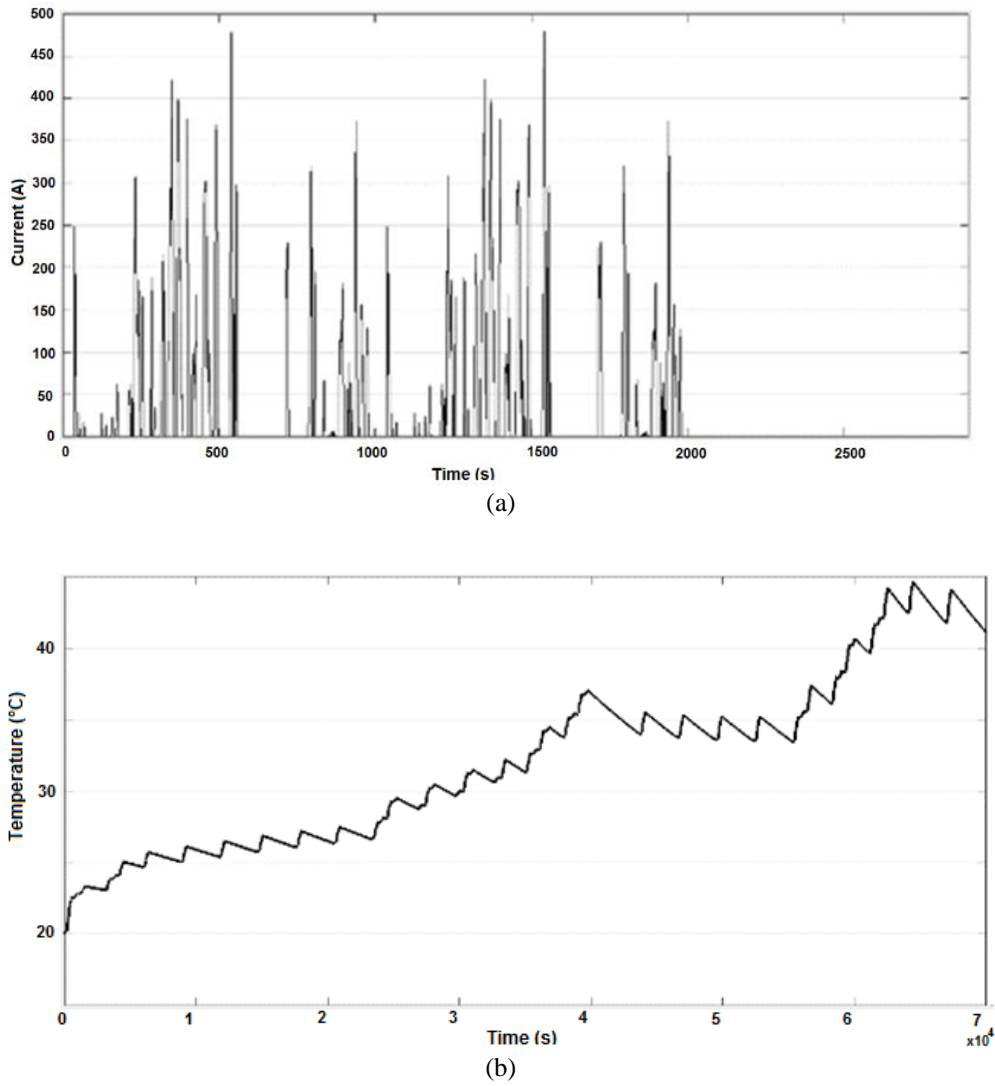


Figure 19. Battery current (a) and Battery temperature (b) ( $E_{\text{Batt}} = 470\text{Ah}$  and  $E_{\text{SC}} = 802\text{Wh}$ )

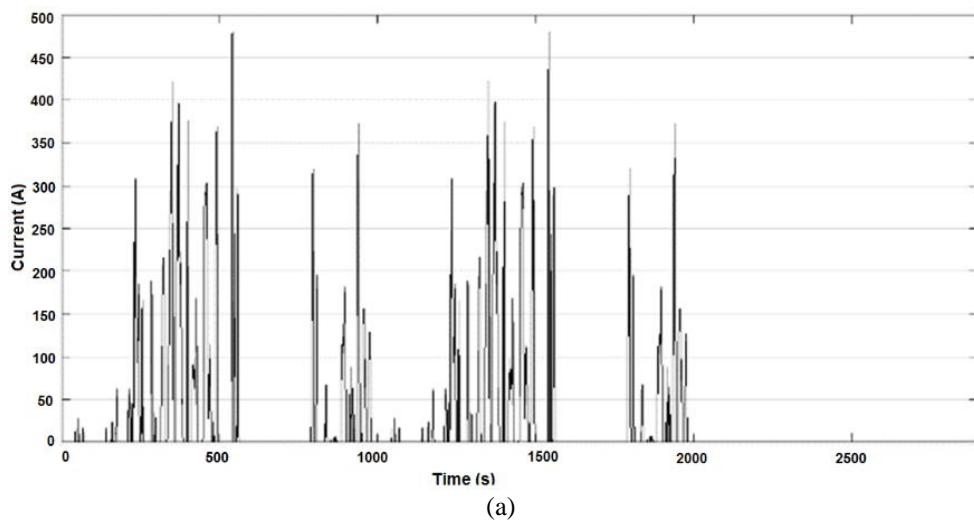


Figure 20. Battery current (a) Battery temperature

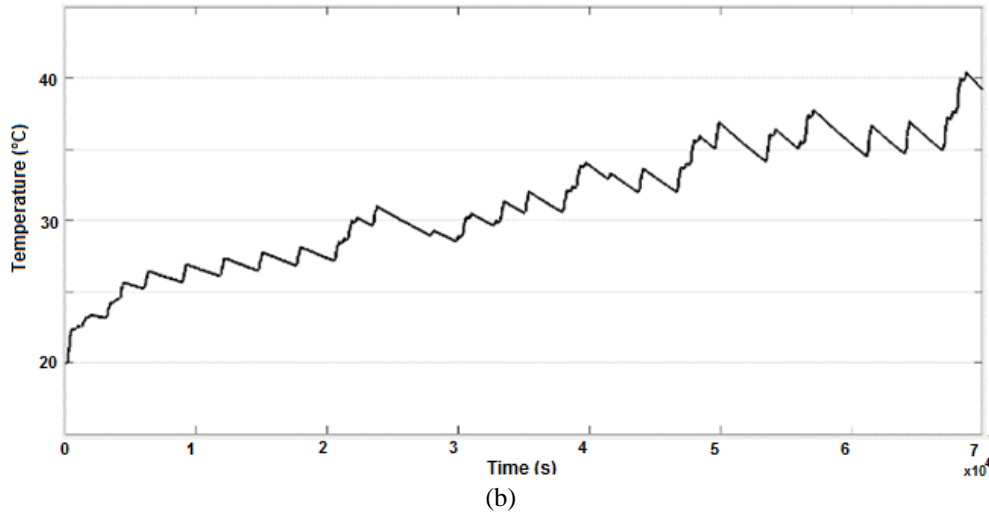


Figure 20. Battery current (b) ( $E_{\text{Batt}} = 389\text{Ah}$  and  $E_{\text{SC}} = 1264\text{Wh}$ ) (*continue*)

The following Table 5 summarizes the results of the simulations performed. We note that from a capacity of 60F we can keep the battery temperature within the allowable limits. For 60F Capacity, the maximum temperature reached is 55°C which is below the battery permissible temperature (60°C). SC energy is about 511 Wh which is 0.16% of the battery energy (330 kWh). With this percentage of hybridization, the battery capacity has been reduced by 32%.

Table 5. Maximum temperature reached for each combination

C (F)	$E_{\text{SC}}$ (Wh)	$E_{\text{Batt}}$ (kWh)	$E_{\text{Batt}} / E$ (%)	T (°C)
0	0	485	100	85
4	34	472	97	80
16	133	439	91	74
60	511	330	68	55
86	744	274	56	50
93	802	262	54	45
146	1264	217	45	40

## 6. CONCLUSION

Based on the ARTEMIS driving cycle and the mechanical parameters of the bus, we calculated the power required for its training system, then we calculated the energy required for its operation during a day. We have determined the optimal share of the energy to be stored in the supercapacitors, to allow the battery to operate in its zone of admissible temperature. The chosen bus case study with a power of 270 kW, requires a daily energy autonomy of 364 kWh is the equivalent of 871 Ah battery under 557 V. We have found the right combination of supercapacitors and batteries, namely 511 Wh for supercapacitors and 592 Ah for battery, which represents 68% of the energy required by the bus. With this combination we have limited the maximum temperature to 55°C.

## ACKNOWLEDGEMENTS

I would like to express here the very thanks to Professors: Mohamed Assini and Abdallah Saad, University Hassan II, who provided me the opportunity to do such a research in their laboratory.

## REFERENCES

- [1] J. Du, F. Li, J. Li, X. Wu, Z. Song, Y. Zou, and M. Ouyang, "Evaluating the technological evolution of battery electric buses: China as a case," *Energy*, vol. 176, no. 1, pp. 309-319, 2019.
- [2] M. Soltani, J. Ronsmans, S. Kakihara, J. Jaguemont, P. Van den Bossche, J. van Mierlo, and N. Omar, "Hybrid battery/lithium-ion capacitor energy storage system for a pure electric bus for an urban transportation application," *Applied Science*, vol. 8, no. 7, pp. 1176-1195, 2018.



- [3] K. Jaewan, O. Jinwoo and L. Hoseong, "Review on battery thermal management system for electric vehicles," *Applied Thermal Engineering*, vol. 149, pp. 192-212, 2019.
- [4] S. M. Faresse, M. Assini, and A. Saad, "Battery thermal behavior in hybrid energy storage unit (battery/supercapacitor) for dynamic loads," *International Journal of Scientific & Engineering Research*, vol. 9, no. 2, pp. 1439-1446, 2018.
- [5] L. Kouchachvili, W. Yaïci, and E. Entchev, "Hybrid battery/supercapacitor energy storage system for the electric vehicles," *Journal of Power Sources*, vol. 374, pp. 237-248, 2018.
- [6] Z. Cabrane, M. Ouassaid, and M. Maaroufi, "Analysis and evaluation of battery-supercapacitor hybrid energy storage system for photovoltaic installation," *International Journal of Hydrogen Energy*, vol. 41, no. 45, pp. 20897-20907, 2016.
- [7] J. Nájera, P. Moreno-Torres, M. Lafoz, R. M. de Castro, and J. R. Arribas, "Approach to hybrid energy storage systems dimensioning for urban electric buses regarding efficiency and battery aging," *Energies*, vol. 10, no. 11, pp. 1708-1724, 2017.
- [8] W. Yusheng, H. Yongxi, X. Jiuping, and N. Barclay, "Optimal recharging scheduling for urban electric buses: A case study in Davis," *Transportation Research Part E*, vol. 100, pp. 115-132, 2017.
- [9] R. Xiong, H. Chen, C. Wang, and F. Sun, "Towards a smarter hybrid energy storage system based on battery and ultracapacitor-a critical review on topology and energy management," *Journal of Cleaner Production*, vol. 202, pp. 1228-1240, 2018.
- [10] S. Zhang, R. Xiong, and X. Zhou, "Comparison of the topologies for a hybrid energy-storage system of electric vehicles via a novel optimization method," *SCIENCE CHINA-Technological Sciences*, vol. 58, no. 7, pp. 1173-1185, 2015.
- [11] T. Zimmermann, P. Keil, M. Hofmann, M. F. Horsche, S. Pichlmaier, and A. Jossen, "Review of system topologies for hybrid electrical energy storage systems," *Journal of Energy Storage*, vol. 8, pp. 78-90, 2016.
- [12] X. Changle, W. Yanzi, H. Sideng and W. Weida, "A New Topology and Control Strategy for a Hybrid Battery-Ultracapacitor Energy Storage System," *Energies*, vol. 7, pp. 2874-2896, 2014.
- [13] S. Ziyou, L. Jianqiu, H. Xuebing, X. Liangfei, L. Languang, O. Minggao and H. Hofmann, "Multi-objective optimization of a semi-active battery/supercapacitor energy storage system for electric vehicles," *Applied Energy*, vol. 135, pp. 212-224, 2014.
- [14] S. Ziyou, H. Hofmann, L. Jianqiu, H. Xuebing, and Z. Xiaowu, "A comparison study of different semi-active hybrid energy storage system topologies for electric vehicles," *Journal of Power Sources*, vol. 274, pp. 400-411, 2015.
- [15] S. Arrigoni, D. Tarsitano, and F. Cheli, "Comparison between different energy management algorithms for an urban electric bus with hybrid energy storage system based on battery and supercapacitors," *Int. J. Heavy Vehicle Systems*, vol. 23, no. 2, pp. 171-189, 2016.
- [16] D. Tarsitano, L. Mazzola, F. Luigi Mapelli, S. Arrigoni, F. Cheli and F. Haskaraman, "On Board Energy Management Algorithm Based on Fuzzy Logic for an Urban Electric Bus with Hybrid Energy Storage System," *Advanced Microsystems for Automotive Applications*, pp. 179-187, 2014.
- [17] Y. Huilong, D. Tarsitano, H. Xiaosong, and F. Cheli, "Real time energy management strategy for a fast charging electric urban bus powered by hybrid energy storage system," *Energy*, vol. 112, pp. 322-331, 2016.
- [18] O. Tremblay and L. A. Dessaint, "Experimental validation of a battery dynamic model for EV applications," *World Electric Vehicle Journal*, vol. 3, no. 2, pp. 289-298, 2009.
- [19] L. H. Saw, K. Somasundaram, Y. Ye, and A.A.O. Tay, "Electro-thermal analysis of lithium iron phosphate battery for electric vehicles," *Journal of Power Sources*, vol. 249, pp. 231-238, 2014.
- [20] P. O. Logerais, M. A. Camara, O. Riou, A. Djellad, A. Omeiri, F. Delaleux, and J. F. Durastanti, "Modeling of a supercapacitor with a multibranch circuit," *International Journal of Hydrogen Energy*, vol. 40, no. 39, pp. 13725-13736, 2015.
- [21] N. Xu and J. Riley, "Nonlinear analysis of a classical system: The double-layer capacitor," *Electrochemistry Communications*, vol. 13, no. 10, pp. 1077-1081, 2011.
- [22] S. N. Motapon, L. A. Dessaint, and K. Al-Haddad, "A comparative study of energy management schemes for a fuel-cell hybrid emergency power system of more-electric aircraft," *IEEE Transactions on industrial electronics*, vol. 61, no. 3, pp. 1320-1334, 2014.
- [23] M. Andre, R. Jourard, R. Vidon, P. Tassel, and P. Perret, "Real-world European driving cycles, for measuring pollutant emissions from high- and low-powered cars," *Atmospheric Environment*, vol. 40, no. 31, pp. 5944-5953, 2006.
- [24] W. Xiaogang, H. Weixiang, and S. Zhibin, "Research on energy management of hybrid energy storage system for electric bus," *Advances in Mechanical Engineering*, vol. 9, no. 10, pp. 1-13, 2017.
- [25] B. Tabbache, S. Djebbari, A. Kheloui, M. Benbouzid, "A Power Presizing Methodology for Electric Vehicle Traction Motors," *International Review on Modelling and Simulations*, vol. 6, pp. 29-32, 2013.
- [26] X. Xin and C. Zhang, "Optimal Design of Electric Vehicle Power System with the Principle of Minimum Curb Mass," *Energy Procedia*, vol. 105, pp. 2629 - 2634, 2017.

**BIOGRAPHIES OF AUTHORS**

**Si Mohamed Faresse** is a Ph.D. student at the National Higher School of Electricity and Mechanics, Laboratory of Electrical Systems and Energy, University Hassan II of Casablanca–Morocco. His research interests include hybrid energy storage system for transport and photovoltaic applications.



**Mohamed Assini**, Ph. D., Professor at the Department of Electrical Engineering, National Higher School of Electricity and Mechanics, University Hassan II of Casablanca, Morocco. His research interests include hybrid energy storage system for transport and photovoltaic applications, Renewable Energies and static converters.



**Abdallah Saad**, Ph. D., Professor at the Department of Electrical Engineering, National Higher School of Electricity and Mechanics, University Hassan II of Casablanca, Morocco. His research interests include hybrid energy storage system for transport and photovoltaic applications, electricity network and Facts, Renewable Energies and smart grids.